Stability of conjugated carbon nanocones

H. Heiberg-Andersen*

Institute for Energy Technology, Physics Department, N-2027, Kjeller, Norway
E-mail: henning.heiberg-andersen@ife.no

A.T. Skjeltorp

Institute for Energy Technology, Physics Department, N-2027, Kjeller, Norway
Department of Physics, University of Oslo, Blindern, N-0316, Oslo, Norway

We use interlacing techniques to prove that carbon nanocones who have a Fries Kekulé structure have closed Hückel shells, and that this result can be extended to all conjugated cones where each edge belongs to a hexagonal face and the configuration of the non-hexagonal faces are consistent with a Fries Kekulé structure. Cones with Fries Kekulé structure or substructure are topical—not only from a valence bond theoretical point of view—since a previous *ab initio* analysis favored cones where the pentagons at the tip are configured as in a Fries Kekulé structure. The question of interdependence will therefore be addressed.

1. Introduction

Carbon nanocones are interesting synthesized [1, 2] structures with subtle electronic properties [3–12] who may be exploited in field emission [9] and scanning tunnelling microscopy [10]. Like the other novel carbon materials, the cones have been considered for hydrogen storage in vehicles. Although the underlying mechanism is not understood, the hydrogen storage characteristics of carbon nanocones encourages further efforts [13]. For any application of the cones, it is significant that an effective production process is already available [2]. This point is of chemiphysical interest too, since cone-shaped molecular structures otherwise rarely appear.

The topology of an open-ended carbon nanocone can be established by cutting 1–5 sectors of angle $60°$ out of a flat hexagonal graphene sheet and joining

*Corresponding author.

the dangling bonds made by the cut. Assuming all bond lengths more or less equal, this gives cone tips with 1–5 pentagonal faces, or alternative structures with the same geometric curvature, implied by the fact that 1 square corresponds to 2 pentagons and 1 triangle corresponds to 3 pentagons, according to Eulers rule. Cones with pentagons at the tip are, however, considered most likely, since faces of shorter length gives larger, and more concentrated, deviations from the optimum $120°$ σ-bond angle.

The procedure described above is usually referred to as 'the pentagon model' in order to distinguish the resulting cones from the conical helical whiskers [16–22] discovered in the late 1960s. The first experimental observation of cones consistent with the pentagon model was published in 1994 [1]. In the hot vapor phase, fullerene cones and open-ended cones were synthesized together with tubes. The fact that all the observed cones had opening angles close to $19°$, which corresponds to five pentagons at the tip, suggested that the tubes (with six pentagons at the capped ends) and the cones grew from similar seeds [14].

Further research was motivated by the simultaneous synthesis of open-ended cones with all the five apex angles consistent with the pentagon model in 1997 [2]. The method used in this experiment is called *Kværner's Carbon-Black* process [15], where the residual hydrogen is recycled during the decomposition of the heavy oil. With the plausible assumption of terminating hydrogens at the open ends, these cones can therefore be understood as π-electronic systems, to which the Hückel theory applies. Despite this, the molecular graphs of carbon nanocones have not attracted the same attention as the fullerene graphs. The study [23–33] of fluoranthenoids (conjugated hydrocarbons composed of one pentagonal ring among otherwise hexagonal rings) and indacenoids (two fused pentagons surrounded by hexagons) that started at the beginning of the 1990s, has proceeded seemingly independent of the discovery of carbon nanocones, as the focus has been on enumeration of isomers.

The majority of the theoretical efforts to understand nanocones, who have been successful indeed, have been devoted to the effects of the pentagons, as topological defects in a graphene sheet, on properties related to potential nano-electronic applications; the local densities of states near the Fermi level [3, 4, 9, 10], local metallization at the tips of cones with $60°$ apex angle (3 pentagons) [7, 11] and the anomalous Aharanov–Bohm effect [6, 7, 11, 12]. In the only systematic work so far entirely concerned with the relative configuration of the pentagons at the tips of nanocones [34], *ab initio* and semi-empirical electronic structure calculations were used to determine the energetically favorable tip topologies, and the results were attributed to minimization of in-plane and out-of-plane strain in the resulting geometries. In this work we will show, among other things, that the favored tip configurations of [34] are imbedded in cone topologies giving properly closed Hückel shells. This raises immediately the question of interdependence, which we shall return to in the concluding section.

2. Hückel theory and curved graphene surfaces

The simple but effective Hückel theory has been an invaluable tool in the study of planar hydrocarbons, largely because it directly invokes the powerful graph theory. A topic that gained new actuality with the discovery of fullerenes and nanotubes, is the applicability of this theory to non-planar graphene surfaces, where the π-orbitals cannot really be regarded as as a linear combination of p-orbitals normal to the sp^2 hybridization plane. A theoretically satisfactory answer, as well as practicable quantitative methods, is given by the work of Haddon [35–37]. He pointed out [35] that the success of the $\sigma - \pi$ separability may be attributed to the *orthogonality* of the σ- and π-orbitals rather than the very concept of σ- and π-electrons who can be treated independent of each other. If accepted as a basic principle, the orbital orthogonality provides an extension of the $\sigma - \pi$ separability to molecules with nuclear coordinates in three dimensions [35], as well as a modified Hückel theory.

In the simplest Hückel theory, the Hamiltonian matrix for the π-orbitals commutes with the adjacency matrix $A(G)$ of the molecular graph G describing the σ framework of the carbons. It is customary to index the n eigenvalues $\theta(A(G))$ of $A(G)$ in non-decreasing order

$$\theta_1(A(G)) \geqslant \theta_2(A(G)) \cdots \geqslant \theta_n(A(G)) \tag{1}$$

and this convention gives the relation

$$\theta_i(A(G)) = \frac{E_i(G) - \alpha}{\beta}, \tag{2}$$

where $E_i(G)$ is the energy of the i'th π-orbital in the Hückel spectrum, α is the (negative) diagonal matrix element of the effective Hamiltonian, called the *Coulumb integral*, and β is the negative [38] resonance integral. In a conjugated carbon molecule n is even, and according to the simplest Hückel theory all bonding π-orbitals are filled (2 electrons in each) and all empty π-orbitals are antibonding if

$$\theta_{n/2}(A(G)) > 0 > \theta_{n/2+1}(A(G)). \tag{3}$$

In Haddon's modified Hückel theory for three dimensions [35] (which is different from the earlier extented-Hückel theory [39] involving all the valence electrons), β is replaced with position dependent scaled resonance integrals in the Hamiltonian matrix. This gives a quantitative improvement of the results at the cost of the correspondence with graph theory expressed by (2) for the simplest Hückel theory. However, since the work of Haddon it is found [40–42] that the geometry itself only has a minor impact on the levels around the Fermi energy for curved carbon surfaces. Since the question of chemical stability is determined by this part of the spectrum, the the graph-theoretical results derived in the following sections will therefore have significance.

3.   Interlacing and Rayleigh's inequalities

If A and B are two symmetric matrices, and their respective eigenvalues $\theta(A)$ and $\theta(B)$ satisfy *Cauchy's inequalities*

$$\theta_i(A) \geqslant \theta_i(B) \geqslant \theta_{i+n-m}(A), \tag{4}$$

where $n \times n$ is the order of A, $m \times m$ is the order of B, and $n \geqslant m \geqslant i$, the eigenvalues of B are said to *interlace* the eigenvalues of A. In this work we will make use of the *Interlacing Theorem* (see, for example, [43] or [44]):

Theorem 1. Let A be a real symmetric n × n matrix and let B be a principal submatrix of A with order m × m. Then, for i = 1, ... , m,

$$\theta_i(A) \geqslant \theta_i(B) \geqslant \theta_{i+n-m}(A). \tag{5}$$

Applied directly to the spectrum of $A(G)$, the adjacency matrix of the molecular graph, this theorem is not strong enough to prove chemically interesting bounds on the eigenvalues. For this we need in addition the powerful interlacing technique based on *Rayleigh's inequalities* [45]:

$$\frac{u^T A u}{u^T u} \geqslant \theta_i(A), \tag{6}$$

where A is a real symmetric matrix and u is a vector in the space spanned by the first i eigenvectors of A, and

$$\frac{v^T A v}{v^T v} \leqslant \theta_{i+1}(A) \tag{7}$$

if v is a vector outside this space.

If A is a real $n \times n$ matrix and R is an $n \times m$ matrix with the property that $R^T R = I$, it is found (see [43] or [46] for details) that Rayleigh's inequalities imply the bounds

$$\theta_i(A) \geqslant \frac{(Rx)^T A R x}{(Rx)^T} \geqslant \theta_i(R^T A R), \tag{8}$$

where x is a nonzero vector with the property that Rx lies outside the space of the first $i - 1$ eigenvalues of A. Since $\theta_i(-A) = -\theta_{n+1-i}(A)$ and $\theta_i(-R^T A R) = -\theta_{m+1-i}(R^T A R)$, (8) implies

$$\theta_i(R^T A R) \geqslant \frac{(Ry)^T A R y}{(Ry)^T} \geqslant \theta_{i+n-m}(A), \tag{9}$$

where y is a nonzero vector and Ry lies outside the space of the last $m - 1$ eigenvalues of A. Summing up, we have, from (8) and (9),

(a) if the $n \times m$ matrix R satisfies $R^T R = I$, the eigenvalues of $R^T A R$ interlace the eigenvalues of the $n \times n$ matrix A, and

(b) if $Au_i = \theta_i(A)u_i$, $R^T A R v_i = \theta_i(R^T A R)v_i$ and $\theta_i(R^T A R) = \theta_i(A)$, then we have the relation $u_i = Rv_i$ between the two eigenvectors, and likewise

(c) if $\theta_i(R^T A R) = \theta_{i+n-m}(A)$, then $u_{i+n-m} = Rv_i$.

This abc is in fact sufficient for proving closed shells of leapfrog fullerenes by the approach of Haemers [46], which is in turn based on the proof of Manolopoulos et al. [47]. The approach of Haemers is also outlined in the excellent book on algebraic graph theory by Godsil and Royle [43].

4. Leapfrog operations and cones with Fries matching

The molecular graphs of conjugated hydrocarbons allow numerous ways to arrange the π-bonds in the old valence bond theory, and each structure formula with a definite arrangement of the π-bonds is called a Kekulé structure. Since each Kekulé structure represents a perfect matching of the n vertices of G, and we will be particularly concerned with the Fries Kekulé structure, we allow ourselves to call it the Fries *matching* and denote it by M. In the early days of organic chemistry, Fries proposed a correlation between the number of benzenoid rings in the structural formula and the stability of the hydrocarbon, and for fullerenes a Fries Kekulé structure is realized when this number attains its maximum of $n/3$ [48]. The analog for the open-ended cones is a matching involving either three or none of the edges of a hexagon, and none of the edges of the smaller faces. Figure 1 shows the tightest possible configuration of 3 pentagons consistent with a Fries matching.
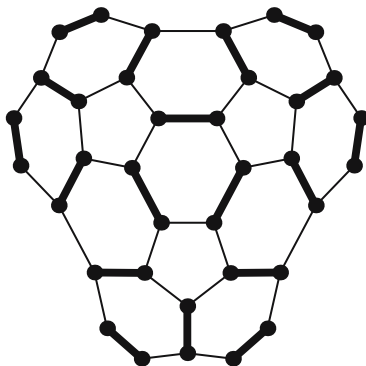

Figure 1. The tightest possible configuration of 3 pentagons consistent with a Fries matching. Edges belonging to the Fries matching are highlighted.

The leapfrog idea was first introduced for closed trivalent carbon clusters (cubic molecular graphs) by Fowler and Steer in [49], and it was later [47] proved rigorously that this operation gives a cubic graph whose adjacency matrix has exactly half of its eigenvalues positive and exactly half of its eigenvalues negative. The technique used in the slightly different route of Haemers [46] is however easier to adapt to open-ended cones, and we will follow his line to set preliminary bounds on $\theta_{n/2}(A(G))$ and $\theta_{n/2+1}(A(G))$ for open-ended cones with Fries matching.

The leapfrog algorithm to be used in this work consists of taking the line graph $L(g)$ of a graph g with outer vertices of valency 1 or 2, and then obtaining G by splitting the vertices of $L(g)$. The procedure is shown in figure 2. It is clear that in general the faces of $L(g)$ consists of the faces of g plus one triangle for each 3-valent vertex of g, and thus every graph G with Fries matching is a leapfrog. However, if there are adjacent 2-valent vertices in g, the leapfrog will not have a Fries matching. This is different from what is the case for cubic graphs, where it can easily be proved [49] that the leapfrog operation implies a Fries matching of the resulting graph.

The important point here is that contraction of the vertices joined by the edges of a Fries matching M gives the line graph $L(g)$, such that

$$B^T(M)A(G)B(M) = 2I + A(L(g)), \tag{10}$$

where $B(M)$ is the $n \times n/2$ vertex-edge (0, 1) incidence matrix of M and $A(L(g))$ is the adjacency matrix of $L(g)$. The adjacency matrix of a line graph and the incidence matrix of the underlying graph are related by the following theorem of Doob (see for example [43] or [44]):

Theorem 2. Let $B(X)$ be the incidence matrix of the graph X, and let L be the line graph of X. Then $B^T(X)B(X) = 2I + A(L)$
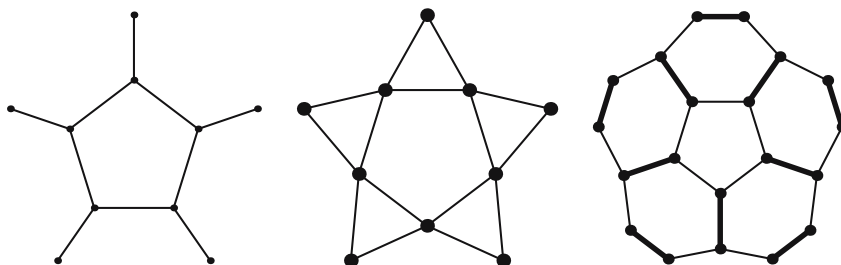

Figure 2. A leapfrog algorithm for hydrocarbons. The highlighted edges in the leapfrog graph to the right indicates the selected splitting of the vertices in the graph in the middle, which in turn is the line graph of the hydrocarbon graph to the left.

This implies that $B^T(M)A(G)B(M)$ is positive semi-definite, and, since the edges of M are non-adjacent, $B^T(M)B(M) = 2I$. Using point (a) of the last section we thus obtain

$$\theta_{n/2}(A(G)) \geqslant \theta_{n/2}\left(\frac{B^T(M)}{\sqrt{2}}A(G)\frac{B(M)}{\sqrt{2}}\right) \geqslant 0 \tag{11}$$

as a preliminary bound on $\theta_{n/2}(A(G))$ for cones with Fries matching. Contracting the edges of any other matching of an open-ended cone will generally lead to a graph having the complete graph $K_{1,3}$—'the claw'—as an induced subgraph near the boundary, and the graph can therefore not be a line graph according to the theorem of Beineke [50].

To establish a chemically interesting bound on $\theta_{n/2+1}(A(G))$ a formal version of the leapfrog operation on cubic graphs was used in [46], and we need to show that an analogous procedure hold for the molecular graphs of hydrocarbons. The leapfrog operation on a cubic graph g can be coded as follows [43, 46]: Let e_i be an edge of g, and let f_j be a face of g that contains e_i. Then the pair $(e_i f_j)$ is a vertex of the leapfrog graph G. If f_j and f_k are two faces containing e_i, the vertices $(e_i f_j)$ and $(e_i f_k)$ are adjacent. If e_i and e_j are two sides of a face f_k, the vertices $(e_i f_k)$ and $(e_j f_k)$ are adjacent if and only if e_i and e_j are adjacent in g. If we relax the concept of 'face' a little bit, we can analogously formalize the leapfrog operation on a graph g with 1-valent vertices along the boundary: We declare the two regions on each side of an edge e_i to be two different faces f_j and f_k. The fact that we can move from one 'face' to another along the boundary of g without crossing any edge does not hamper this algorithm, and the edges of the Fries matching M of G now connects the 'faces' of g.

Following [46] we now give the edges of M an arbitrary orientation and let $D(M)$ be the $(0, \pm 1)$ incidence matrix of the oriented edges; the nonzero entries $(D(M))_{VE}$ are positive if the orientation of the edge E points *from* the vertex V to the opposite end vertex of E, and negative if the orientation points *against* V. Let us now calculate the various entries of $D^T(M)A(G)D(M)$. If we let $V_1(E)$ and $V_2(E)$ denote respectively the vertices on which $(D(M))_{VE}$ are positive and negative, we see that the diagonal entries are identical:

$$\begin{aligned}
(D^T(M)A(G)D(M))_{EE} &= \sum_{V'V}(D^T(M))_{EV'}(A(G))_{V'V}(D(M))_{VE} \\
&= 2(D^T(M))_{EV_1(E)}(D(M))_{V_2(E)E} \\
&= -2.
\end{aligned} \tag{12}$$

For the non-diagonal entries, at most one of the four terms in the sum

$$(D^T(M)A(G)D(M))_{E'E} = \sum_{V'V}(D^T(M))_{E'V'}(A(G))_{V'V}(D(M))_{VE} \tag{13}$$

is nonzero. This follows from the fact that each edge of M is one of three sides of a hexagon in G, so two different edges of M is connected by at most one edge (which is not part of M). According to the formal leapfrog operation, the edges of M connect the 'faces' of g, and can be written $E = ((e_i f_j), (e_i f_k))$ so the non-zero non-diagonal entries have the form

$$(D^T(M)A(G)D(M))_{((e_i f_j),(e_i f_k)),((e_i f_j),(e_l f_m))}$$
$$= (D^T(M))_{(e_i f_j),((e_i f_j),(e_i f_k))}(D(M))_{(e_l f_j),((e_l f_j),(e_l f_m))}, \tag{14}$$

where e_i and e_l are adjacent edges in a face of g. The $(e_i e_j)$ entry of $d^T(g)d(g)$, where $d(g)$ is the incidence matrix for an orientation of g, is given by

$$(d^T(g)d(g))_{e_i e_j} = (d(g))_{v_1(e_i)e_l} - (d(g))_{v_2(e_i)e_l}, \tag{15}$$

where $v_1(e_i)$ and $v_2(e_i)$ are respectively the vertices of g where the entries $d(g)_{v,e_i}$ are positive and negative. If we orient the edges $E = ((e_i f_j), (e_i f_k))$ of M so that $V_1(E) = (e_i f_j)$ if f_j is on the right (or left) when we walk along e_i in the direction specified by the orientation of g, we get

$$(D^T(M)A(G)D(M))_{((e_i f_j),(e_i f_k)),((e_l f_j),(e_l f_m))} = -(d^T(g)d(g))_{e_i e_j} \tag{16}$$

both if f_j is on the right/left of e_i and e_l and if f_j is on the right/left of e_i and on the left/right of e_l as we walk in the direction specified by the orientation of g. A straightforward calculation gives $(d^T(g)d(g))_{e_i e_i} = 2$, so, collecting results gives

$$D^T(M)A(G)D(M) = -d^T(g)d(g), \tag{17}$$

and $D^T(M)A(G)D(M)$ is thus negative semidefinite. As for $B(M)$, we get $D^T(M)D(M) = 2I$, and we can again apply point (a) of the last section to obtain the preliminary bound

$$0 \geqslant \theta_1\left(\frac{D^T(M)}{\sqrt{2}}A(G)\frac{D(M)}{\sqrt{2}}\right) \geqslant \theta_{n/2+1}(A(G)) \tag{18}$$

which makes the first unoccupied Hückel orbital either non-bonding ($\theta = 0$) or anti-bonding ($\theta < 0$).

5.   Conjugated subgraphs of cones with Fries matching

We will now show that the preliminary eigenvalue bounds of the last section hold also for conjugated induced subgraphs, without Fries matchings, of the cone graphs with Fries matchings. Let G be the molecular graph of a cone with Fries matching. Then there exist two complementary induced subgraphs G_1 and G_2 on n_1 and n_2 even numbers of vertices. Since each row of $B(M)$, the incidence

matrix of the Fries matching M of G, has exactly one non-zero entry, the incidence matrix of any other perfect matching of G is obtained by permuting the rows of $B(M)$. Since all graphs with even number of vertices have perfect matchings, there is a perfect matching $M' \equiv M_1 + M_2$ of G where M_1 and M_2 are perfect matchings of G_1 and G_2, and

$$B(M') = \Pi B(M), \tag{19}$$

where Π is a row permutation operator;

$$\Pi = \Pi_{1i} \Pi_{2j} \Pi_{3k} \dots , \tag{20}$$

where Π_{1i} permutes the first and the i'th row, Π_{2j} permutes the second and the j'th row, and so on, such that the two nonzero entries of each column of $B(M')$ are located at the rows corresponding to the vertices connected by the edge of M' corresponding to the actual column. This gives

$$B^T(M')A(G)B(M') = B^T(M)(\dots \Pi_{3k}\Pi_{2j}\Pi_{1i})A(G)(\Pi_{1i}\Pi_{2j}\Pi_{3k}\dots)B(M)$$
$$= B^T(M)A(G)B(M) \tag{21}$$

since the permutation operations performed on $A(G)$ from the left side are reversed from the right side, so $B^T(M')A(G)B(M')$ is positive semidefinite according to (11). If we replace $B(M')$ with $B(M' - M_2)$, the matrix obtained by deleting all columns corresponding to edges in M_2 from $B(M')$, in (21), we obtain

$$B^T(M_1)A(G_1)B(M_1) = B^T(M' - M_2)A(G)B(M' - M_2) \tag{22}$$

as a principal submatrix of $B^T(M')A(G)B(M')$, since $A(G_1)$ is a principal submatrix of $A(G)$, and none of the edges of M' connect G_1 and G_2. The second inequality of Theorem 1 then gives

$$\theta_{n_1/2}(B^T(M_1)A(G_1)B(M_1)) \geqslant \theta_{(n_1+n_2)/2}(B^T(M')A(G)B(M')) \geqslant 0, \tag{23}$$

and we can once again apply point (a) in Section 2 to obtain the bound

$$\theta_{n_1/2}(A(G_1) \geqslant \theta_{n_1/2}\left(\frac{B^T(M_1)}{\sqrt{2}}A(G_1)\frac{B(M_1)}{\sqrt{2}}\right) \geqslant 0 \tag{24}$$

for any conjugated induced subgraph of a cone graph with Fries matching.

The permutation procedure followed by column deletion applies also to the incidence matrix of the oriented Fries matching, $D(M)$, and the first inequality of Theorem 1 gives

$$\theta_1(D^T(M)A(G)D(M)) \geqslant \theta_1(D^T(M_1)A(G_1)D(M_1)), \tag{25}$$

so $D^T(M_1)A(G_1)D(M_1)$ is negative semidefinite, and we get

$$0 \geqslant \theta_1 \left(\frac{D^T(M_1)}{\sqrt{2}} A(G_1) \frac{D(M_1)}{\sqrt{2}} \right) \geqslant \theta_{n_1/2+1}(A(G_1)) \qquad (26)$$

when G_1 and G are specified as above.

6. Closing the Hückel shells

In the last two sections we have established the preliminary bounds

$$\theta_{n/2}(A(G)) \geqslant 0 \geqslant \theta_{n/2+1}(A(G)) \qquad (27)$$

both for cones with Fries matching and for their induced conjugated subgraphs, and closed Hückel shells are guaranteed for the cases where the equalities of (27) can be eliminated. From the structure of the adjacency matrix of a graph without loops or multiple edges it follows that for any vertex of the graph, the sum of the components of the eigenvector on the adjacent vertices is equal to the eigenvalue multiplied by the component on the actual vertex (see for example [43]). Thus, if

$$(A(G))u = 0 \qquad (28)$$

shall have a solution for a nonzero eigenvector u, this eigenvector must sum to zero on all neighbors of any vertex without having all components equal to zero. This fact, together with point (b) and (c) of Section 2, was used in the proof of the eigenvalue theorem for leapfrogs of cubic graphs [46, 47]. However, this proof involves the fact that each edge of the Fries matching then belongs to two hexagons, and since this is not the case for the cones, we need to show explicitly that (28) has only the trivial solution for cones with Fries matching. Thereafter we will be able to close the Hückel shells also for a large fraction of the subgraphs.

6.1. Cones with Fries matching

Assume $A(G)u_{n/2} = 0$. Then, according to (11) and point(b) of Section 2, there is a vector $v_{n/2}$ such that

$$\frac{B^T(M)}{\sqrt{2}} A(G) \frac{B(M)}{\sqrt{2}} v_{n/2} = 0 \qquad (29)$$

and

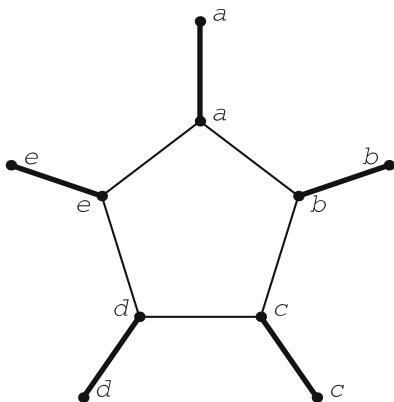$$u_{n/2} = \frac{B(M)}{\sqrt{2}} v_{n/2} \qquad (30)$$

Figure 3. The assumed eigenvector to $\theta_{n/2}(A(G)) = 0$ at a pentagon.

which means that the components of $u_{n/2}$ must be equal on two vertices connected by an edge of M. In figure 3, the components of a vector satisfying this restriction on a pentagon is denoted by the letters a to e. To simultaneously satisfy (28) these components must obey the equations

$$a + b + e = 0$$
$$b + a + c = 0$$
$$c + b + d = 0$$
$$d + c + e = 0$$
$$e + a + d = 0$$

which has $a = b = c = d = e = 0$ as the only solution. We see from figure 4 that this also implies that the eigenvector is zero on the adjacent hexagons, which in turn implies three components equal to zero in the hexagons linked to the pentagon by edges of the Fries matching as shown in figure 5. Solving the equations for the remaining components of this hexagon, labeled q, r and s, gives $q = r = s = 0$, and so on. If a 2-valent vertex at the boundary of the cone is adjacent to a vertex on which $u_{n/2}$ is zero, $u_{n/2}$ must be zero on the other neighbor too, so (28) has no non-trivial solution for $u_{n/2}$. This reasoning applies if the pentagons are replaced by other faces of odd length too, so $\theta_{n/2}(A(G)) > 0$ for cones with pentagons and/or triangles at the tip, if they have a Fries matching.

Assume $A(G)u_{n/2+1} = 0$. Then, according to point (c) of Section 2, there is a vector v_1, such that

$$u_{n/2+1} = \frac{D(M)}{\sqrt{2}} v_1 \tag{31}$$

which means that $u_{n/2+1}$ sums to zero on two vertices connected by an edge of M. The equations for the components on a pentagon are in this case (see figure 6)
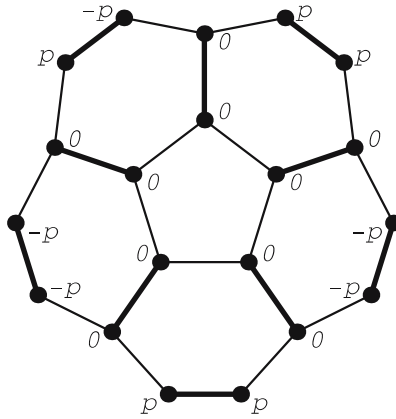
Figure 4. The assumed eigenvector to $\theta_{n/2}(A(G)) = 0$ around a pentagon.
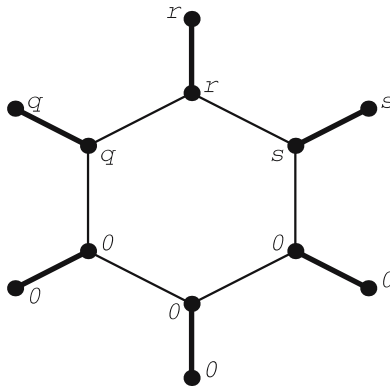

Figure 5. The assumed eigenvector to $\theta_{n/2}(A(G)) = 0$ at a hexagon linked to a pentagon or a triangle by an edge of M.

$$-a + b + e = 0$$
$$-b + a + c = 0$$
$$-c + b + d = 0$$
$$-d + c + e = 0$$
$$-e + a + d = 0$$

with solution $a = b = c = d = e = 0$. It can be shown [47] that $u_{n/2+1}$ must be zero on all faces not divisible by 6 if the graph has a Fries matching, so the result we will get for $\theta_{n/2+1}(A(G))$ is valid for cones with only squares at the tip too. In figure 7 we denote the components of $u_{n/2+1}$ on a hexagon linked by an edge of M to a face not divisible by 6 by the letters p to s. Solving equations analogous to those above, gives $r = 0$ and $p = q = -s$. Since $r = 0$, the same
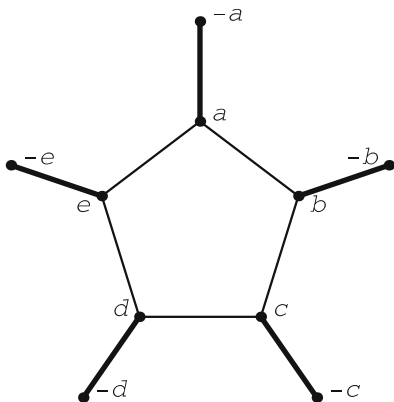
Figure 6. The assumed eigenvector to $\theta_{n/2+1}(A(G)) = 0$ at a pentagon.
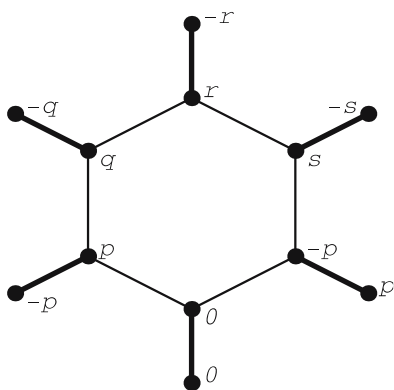

Figure 7. The assumed eigenvector to $\theta_{n/2+1}(A(G)) = 0$ at a hexagon linked by an edge of M to a face not divisible by 6.

set of equations must be satisfied for each hexagon without edges in M. At the boundary this implies adjacent hexagons with 3 edges in M where the components of $u_{n/2+1}$ are equal to zero on each vertex. This in turn gives additional zero-valued components in hexagons without edges in M, where the above mentioned equation set then requires zero-valued components on all vertices of these hexagons, so finally each component of $u_{n/2+1}$ must be zero if $\theta_{n/2+1}(A(G)) = 0$.

Now it is proved that

$$\theta_{n/2}(A(G)) > 0 > \theta_{n/2+1}(A(G)) \tag{32}$$

for all cones with Fries matching and one or more faces of odd length at the tip. Cones with one or two squares, and no pentagons or triangles, have bipartite graphs and are thus subjected to the *Pairing Theorem* [51] of Coulson and Rushbroke, stating that $\theta_i(A(G)) = -\theta_{n+1-i}(A(G))$ for an even bipartite graph
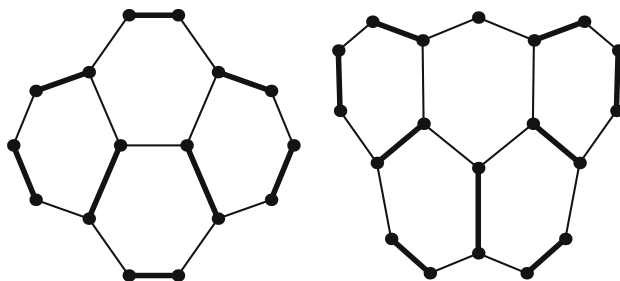
Figure 8. Boundary topologies of cones having induced subgraphs with Fries matching.

G. Therefore, since $0 > \theta_{n/2+1}(A(G))$ for cones having a face not divisible by 6 and a Fries matching, (32) holds for these species too.

6.2. Cones with Fries matching of induced subgraphs

We restrict the further analysis to conjugated cones where each edge of the molecular graph belongs to a hexagonal face, and the configuration of the non-hexagonal faces is consistent with a Fries matching. If a conjugated cone without Fries matching has an induced subgraph with Fries matching, the boundary topologies will be as shown in figure 8; two adjacent 2-valent vertices who are not part of the Fries matching (left), and/or a single 2-valent vertex (right) between two hexagons, each having 3 edges in M. The latter can only appear an even number of times in a conjugated cone graph, since n is then even. In the first case it is easy to see that $u_{n/2}$ and $u_{n/2+1}$ must be zero on the two adjacent vertices outside the Fries matching, since both vectors are zero on neighbors in M. In the second case it is always possible to make a matching covering the isolated vertices by a rearrangement involving only the edges of M near the boundary of the cone, so that the 2-valent vertices connected by edges in the new matching have neighbors on which $u_{n/2}$ and $u_{n/2+1}$ are zero, and the equalities of (27) are eliminated also for this subclass of cones.

7. Summary and conclusions

Via a leapfrog algorithm for hydrocarbons we have used interlacing and the structure of the adjacency matrix to show that all carbon nanocones with Fries matching have closed Hückel shells. Our main line of attack is the same as the one used by other authors for the leapfrog fullerenes. Contrary to what is the case for the fullerenes, we have shown that the results obtained for the leapfrog cones can be significantly extended: The preliminary bounds on the eigenvalues hold for all conjugated carbon nanocones whose molecular graphs are induced subgraphs of cones with Fries matching, and the Hückel shells are strictly closed

for cones where each edge belongs to a hexagonal face and the configuration of the non-hexagonal faces is consistent with a Fries matching.

These cones are favored also by valence bond theory, since the possibility to keep all double bonds outside the non-hexagonal faces suppresses the Mills–Nixon effect [52, 53]. This brings us to the question about the coincidence between these topologies and the pentagon configurations favored by the *ab initio* energy calculations of [34]. By computing the Hückel spectra of the isomers compared in that work, we find that only in the case of two pentagons have both systems closed Hückel shells. For three pentagons a C_{3v}-symmetric $C_{40}H_{12}$ tip, which has an induced subgraph with Fries matching and thus closed shells, is compared with a degenerate isomer with $\theta_{20} = \theta_{21} = 0.182$. In the latter case the two last electrons can be distributed over the two degenerate states in four possible ways; three singlets and one triplet state. In the analogous case of the pseudo-aromatic $C_{4n}H_{4n}$ molecules these states are split by Coulomb repulsion and static bond alternation occur [54, 55]. If the same happens to the above mentioned isomer, the valence bond picture can be invoked, and it is readily understood that it is unfavored since some double bounds need to pass through the pentagons of this configuration. However, without a complementary study of the vibrational spectrum, it cannot be decided if such a static deformation is real or if the underlying Born–Openheimer approximation breaks down. In our opinion, questions of this type are now of secondary interest for the cones, and our further theoretical efforts will be focused on the large fraction of closed-shell topologies unveiled in this work.

Acknowledgments

References

[1] M. Ge and K. Sattler, Chem. Phys, Lett. 220 (1994) 192.
[2] A. Krishnan, E. Dujardin, M.M.J. Treacy, J. Hugdahl, S. Lynum and T.W. Ebbesen, Nature 388 (1997) 451.
[3] R. Tamura and M. Tsukada, Phys. Rev. B 49 (1994) 7967.
[4] R. Tamura, K. Akagi, M. Tsukada, S. Itoh and S. Ihara, Phys. Rev. B 56 (1997) 1404.
[5] K. Kobayashi, Phys. Rev. B 61 (2000) 8496.
[6] P.E. Lammert and V.H. Crespi, Phys. Rev. Lett. 85 (2000) 5190.
[7] V.A. Osipov and E.A. Kochetov, JETP Lett. 73 (2001) 562.
[8] T. Yamaguchi, Surf. Sci. 493 (2001) 597.
[9] J.-C. Charlier and G.-M. Rignanese, Phys. Rev. Lett. 86 (2001) 5970.
[10] O.A. Shenderova, B.L. Lawson, D. Areshkin and D.W. Brenner, Nanotechnology 12 (2001) 191.
[11] V.A. Osipov, E.A. Kochetov and M. Pudlak, J. Exp. Theor. Phys. 96 (2003) 140.
[12] P.E. Lammert and V.H. Crespi, Phys. Rev. B 69 (2004) 035406.

[13] US Patent No. 6,290,753 B1 issued Sept. 18, 2001, to A. T. Skjeltorp and A. Maeland.
[14] K. Sattler, Carbon 33 (1995) 915.
[15] Kværner's patent no PCT/NO98/00093 for production of micro domain particles by use of a plasma process.
[16] M.G. Day, B.C.I.R.A. Jl. 18 (1970) 17.
[17] B. Lux, M. Grages and D. Sapey, Prakt. Metallogr. 5 (1968) 587.
[18] B. Lux, W. Bollmann and M. Grages, Prakt. Metallogr 6 (1969) 530.
[19] M.B. Haanstra, W.F. Knippenberg and G. Verspui, J. Crystal Growth 16 (1972) 71.
[20] D.D. Double and A. Hellawell, Acta Metall. 17 (1969) 1071.
[21] D.D. Double and A. Hellawell, Acta Metall. 19 (1971) 1303.
[22] D.D. Double and A. Hellawell, Acta Metall. 22 (1974) 481.
[23] J.R. Dias, Chem. Phys. Lett. 185 (1991) 10.
[24] J.R. Dias, Chem. Phys. Lett. 187 (1991) 334.
[25] J.R. Dias, J. Chem. Inf. Comput. Sci. 32 (1992) 2.
[26] J.R. Dias, J. Chem. Inf. Comput. Sci. 32 (1992) 203.
[27] J.R. Dias, J. Chem. Inf. Comput. Sci. 35 (1992) 148.
[28] S.J. Cyvin, J. Mol. Struct. 262 (1992) 219.
[29] S.J. Cyvin, B.N. Cyvin and J. Brunvoll, J. Mol. Struct. 281 (1993) 229.
[30] S.J. Cyvin, B.N. Cyvin, J. Brunvoll, Z. Fuji, G. Xiaofeng and R. Tosic, J. Mol. Struct. 285 (1993) 179.
[31] J. Brunvoll, B.N. Cyvin, S.J. Cyvin, G. Brinkmann and J. Bornhoft, Z. Naturforsch. 51a (1996) 1073.
[32] J. Brunvoll, B.N. Cyvin and S.J. Cyvin, J. Chem. Inf. Comput. Sci. 36 (1996) 91.
[33] G.G. Cash and J.R. Dias, Z. Naturforsch. 57a (2002) 650.
[34] J. Han and R. Jaffe, J. Chem. Phys. 108 (1998) 2817.
[35] R.C. Haddon, Acc. Chem. Res. 21 (1988) 243.
[36] R.C. Haddon, Acc. Chem. Res. 25 (1992) 143.
[37] R.C. Haddon, Science 261 (1993) 1545.
[38] J.N. Murrell, S.F.A. Kettle and J.M. Tedder, *The Chemical Bond* (Wiley, New York, 1978).
[39] R. Hoffmann, J. Chem. Phys. 39 (1963) 1397.
[40] J.W. Mintmire, B.I. Dunlap and C.T. White, Phys. Rev. Lett. 68 (1992) 631.
[41] K. Akagi, R. Tamura, M. Tsukada, S. Itoh and S. Ihara, Phys. Rev. Lett. 74 (1995) 2307.
[42] M.S. Dresselhaus, G. Dresselhaus and P.C. Eklund *Science of Fullerenes and Carbon Nanotubes* (Academic Press, 1995).
[43] C. Godsil and G. Royle, *Algebraic Graph Theory* (Springer-Verlag, 2001).
[44] D.M. Cvetković, M. Doob and H. Sachs, *Spectra of Graphs* (Academic Press, 1980).
[45] S.H. Gould, *Variational Methods for Eigenvalue Problems* (Oxford University Press, Oxford, 1966).
[46] W.H. Haemers, Linear Algebra Appl. 226/228 (1995) 593.
[47] D.E. Manolopoulus, D.R. Woodall and P.W. Fowler, J. Chem. Soc. Faraday Trans. 88 (1992) 2427.
[48] P.W. Fowler, J. Chem. Soc. Perkin Trans. 2 (1992) 145.
[49] P.W. Fowler and J.I. Steer, J. Chem. Soc., Chem. Commun. (1987) 1403.
[50] L. Beineke, *Derived Graphs and Digraphs in Beiträge zur Graphentheorie* (Teubner, Leipzig, 1968).
[51] C.A. Coulson and G.S. Rushbroke, Proc. Cambridge, Phil. Soc. 36 (1940) 193.
[52] W.H. Mills and I.G. Nixon, J. Chem. Soc. (1930) 2510.
[53] R. Taylor and D.R.M. Walton, Nature 363 (1993) 685.
[54] L.C. Snyder, J. Phys. Chem. 66 (1962) 2299.
[55] L. Salem, *The Molecular Orbital Theory of Conjugated Systems* (W.A. Benjamin, Reading, 1966).